Neuroscience 356 (2017) 242–254

NICOTINE-INDUCED AND D1-RECEPTOR-DEPENDENT DENDRITIC REMODELING IN A SUBSET OF DORSOLATERAL STRIATUM MEDIUM SPINY NEURONS

DANIEL G. EHLINGER,[a†] JULIAN C. BURKE,[b†] CRAIG G. MCDONALD,[b] ROBERT F. SMITH[b] AND HADLEY C. BERGSTROM[c*]

[a] *Department of Anesthesiology, Perioperative and Pain Medicine, Boston Children's Hospital, Harvard Medical School, Boston, MA, USA*

[b] *Department of Psychology, George Mason University, Fairfax, VA, USA*

[c] *Department of Psychological Science, Program in Neuroscience and Behavior, Vassar College, Poughkeepsie, NY, USA*

Abstract—Nicotine is one of the most addictive substances known, targeting multiple memory systems, including the ventral and dorsal striatum. One form of neuroplasticity commonly associated with nicotine is dendrite remodeling. Nicotine-induced dendritic remodeling of ventral striatal medium spiny neurons (MSNs) is well-documented. Whether MSN dendrites in the dorsal striatum undergo a similar pattern of nicotine-induced structural remodeling is unknown. A morphometric analysis of Golgi-stained MSNs in rat revealed a natural asymmetry in dendritic morphology across the mediolateral axis, with larger, more complex MSNs found in the dorsolateral striatum (DLS). Chronic nicotine produced a lasting (at least 21 day) expansion in the dendritic complexity of MSNs in the DLS, but not dorsomedial striatum (DMS). Given prior evidence that MSN subtypes can be distinguished based on dendritic morphology, MSNs were segregated into morphological subpopulations based on the number of primary dendrites. Analysis of these subpopulations revealed that DLS MSNs with more primary dendrites were selectively remodeled by chronic nicotine exposure and remodeling was specific to the distal-most portions of the dendritic arbor. Co-administration of the dopamine D1 receptor (D1R) antagonist SCH23390 completely reversed the selective effects of nicotine on DLS MSN dendrite morphology, supporting a causal role for dopamine signaling at D1 receptors in nicotine-induced dendrite restructuring. Considering the functional importance of the DLS in shaping and expressing habitual behavior, these data support a model in which nicotine induces persistent and selective changes in the circuit connectivity of the DLS that may promote and sustain addiction-related behavior.

Key words: addiction, habit, direct pathway, indirect pathway, plasticity, adolescence.

INTRODUCTION

Nicotine is a potent reinforcing stimulus, making it among the most addictive substances known (Pontieri et al., 1996). The progression from casual to compulsive drug use is thought to be mediated by mechanisms of neuronal plasticity that underlie normative learning and memory processes (Hyman, 2005). Nicotine targets multiple memory systems associated with reward learning, including the striatum (Rice and Cragg, 2004). The striatum is positioned at the center of cortico-basal ganglia loops that integrate a wide range of input necessary for reinforcement learning, decision-making and motor control (Graybiel, 2000). The striatum is broadly defined along the dorsal and ventral axis (Voorn et al., 2004), with the ventral striatum being the most intensely studied striatal region in the context of reinforcement learning and addiction (Everitt and Robbins, 2005). However, the dorsal striatum also critically participates in reinforcement learning, including decision-making related to action selection (Balleine et al., 2007).

While the ventral striatum is an established target for neuroadaptations in response to nicotine (Koob and Volkow, 2010), nicotine also induces neuroplasticity in the dorsal striatum (Valjent et al., 2004; Pascual et al., 2009; Ortega et al., 2013; Clemens et al., 2014). The dorsal striatum is anatomically and functionally segregated into medial and lateral zones. During the course of instrumental learning, one model suggests the acquisition of goal-directed action selection initially mediated by the DMS is gradually taken over by the dorsolateral striatum (DLS) and expressed as habits (Yin et al., 2004, 2006; Balleine and O'Doherty, 2010). As addiction has been conceptualized as a transition from voluntary consumption to compulsive habit, with a loss of control over drug intake in the face of negative consequences (Belin et al., 2009), a shift in neuronal control from DMS to DLS could underlie the progression from voluntary to habitual drug intake (Yin et al., 2004; Corbit et al., 2012; Gremel and Lovinger, 2016).

One exceptionally persistent form of neuroplasticity commonly associated with addictive drug exposure is dendritic remodeling (Robinson and Kolb, 2004). Nicotine-induced dendritic remodeling in the ventral

*Corresponding author.
E-mail address: habergstrom@vassar.edu (H. C. Bergstrom).
† Denotes equal contribution to the article.
Abbreviations: BAC, bacterial artificial chromosome; D1R, dopamine D1 receptor; DLS, dorsolateral striatum; DMS, dorsomedial striatum; MSNs, medium spiny neurons; PCA, principal components analysis.

http://dx.doi.org/10.1016/j.neuroscience.2017.05.036
0306-4522/

striatum is well-documented (Brown and Kolb, 2001; Hamilton and Kolb, 2005) and is particularly pronounced when exposure occurs during adolescence (McDonald et al., 2007). Furthermore, systemic blockade of dopamine 1 (D1) receptors during nicotine exposure in the adolescent brain completely blocks nicotine-induced dendrite remodeling in the ventral striatum (Ehlinger et al., 2016), suggesting a causal role for dopaminergic signaling at D1 receptors in nicotine-induced dendritic plasticity in the ventral striatum. Comparable measures in the dorsal striatum are lacking. To address this research gap, the dendritic morphology of Golgi-stained medium spiny neurons (MSNs) in the DMS and DLS were completely reconstructed in three-dimensions and morphometrically analyzed after a chronic systemic intermittent nicotine regimen (subcutaneous 0.5 mg/kg, 2 weeks, 8 total injections) during adolescence (PN28-42) in male Sprague-Dawley rats, with or without, co-administration of the highly selective D1 receptor antagonist SCH23390 (subcutaneous 0.05 mg/kg). Because addiction is also defined by chronic relapse (NIDA, 2014), it is important to identify long-lasting changes in cellular plasticity following drug exposure (Grueter et al., 2012), therefore dendritic morphology was measured at a protracted time frame (21-days) following the end of nicotine exposure.

Striatal MSNs can be divided into distinct subpopulations based on anatomical connectivity (i.e., striatonigral ‘‘direct” and striatopallidal ‘‘indirect” pathways), molecular composition (i.e., D1- and D2-expressing) and functionality (Kreitzer and Malenka, 2008; Kravitz et al., 2012). Recent evidence suggests that striatal MSNs can also be divided into distinct *morphological* subpopulations (Gertler et al., 2008; Gagnon et al., 2017). Whether nicotine selectively influences the dendritic branching pattern of these morphologically defined MSN subpopulations has not been analyzed. MSNs were segregated into subpopulations based on the number of primary dendrites (first order dendrites emanating from the soma). The use of primary dendrites as a criterion structural feature for segregating MSN subpopulations is advantageous in the context of nicotine exposure, as nicotine does not influence this particular feature of MSN morphology (Brown and Kolb, 2001; McDonald et al., 2005, 2007; Hamilton and Kolb, 2005; Ehlinger et al., 2012) and primary dendrite number has been shown previously to differentiate striatal MSN cell types (Gertler et al., 2008). DMS and DLS MSN dendritic remodeling in response to nicotine with or without D1 antagonist co-administration was characterized within morphologically subdivided ‘‘large” and ‘‘small” subpopulations, based on primary dendrite number.

Our results reveal (1) a naturally existing asymmetry in MSN dendrite morphology between the DLS and DMS, (2) a lasting (at least 21 days) increase in the dendritic complexity of MSNs in the DLS, but not DMS, following chronic nicotine exposure, (3) selective dendritic remodeling for a morphological distinct DLS MSN subpopulation that contains more primary dendrites (large subpopulation), and (4) a blockade of this structural plasticity when animals are co-administered the D1 antagonist SCH23390 during nicotine exposure. Collectively, these results suggest a selective, persistent, and D1 receptor-dependent influence of chronic nicotine on a morphologically discrete DLS MSN subpopulation.

EXPERIMENTAL PROCEDURES

Animals

All data analyzed in this study were derived from tissue generated using experimental procedures that were described in detail in a previously published study (Ehlinger et al., 2016). Male Sprague-Dawley rats (N = 32) (Harlan, IN, USA) arrived to the vivarium at PN21, were housed in groups (n = 3–4) in standard caging, and allowed *ad libitum* access to food and water. The vivarium was controlled for temperature, humidity and light cycle. All experimental procedures were carried out in accordance with the National Research Council Guide for the Care and Use of Laboratory Animals and the George Mason University IACUC. Disclosure of housing and husbandry procedures was in accordance with recommendations for standard experimental reporting in behavioral neuroscience research (Prager et al., 2011).

Drugs and injection schedule

(-)-Nicotine hydrogen tartrate (Nicotine; Sigma Aldrich, St. Louis, MO, USA) was dissolved in 0.9% saline and administered at a dose of 0.5 mg/kg. R(+)-SCH-23390 hydrochloride (SCH-23390; Sigma Aldrich, St. Louis, MO, USA) was dissolved in 0.9% saline and administered at a dose of 0.05 mg/kg. Physiological saline (0.9% NaCl) was the vehicle control. All drugs were administered subcutaneously at a volume of 1 mL/kg. Drugs were administered during adolescence (PN28-42) in rats that were randomly assigned to one of four pretreatment-treatment groups (n = 8 per group): (1) vehicle-vehicle, (2) SCH-23390-vehicle, (3) vehicle-nicotine or (4) SCH-23390-nicotine. The pretreatment drug (vehicle or SCH-23390) was administered exactly 20 min prior to the treatment drug (vehicle or nicotine). Animals were dosed intermittently in their home-cage every other day during an adolescent (PN28-42) timeframe (eight total injections). Rats were grouped housed throughout the course of the study, eliminating isolation-induced stress effects.

Golgi-stain

Prior to Golgi staining there were 21 drug-free days (PN42-63). On PN63, rats were anesthetized with a ketamine/xylazine cocktail and then perfused intracardially with 0.9% saline. The whole brain was placed into a Golgi solution (mercuric chloride, potassium chromate, and potassium dichromate) and stored in the dark at room temperature for 14 days (Golgi solution refreshed after two days). Brains were then transferred into a 30% sucrose solution for three days prior to sectioning. Brains were sectioned (200 μm; coronal) on a vibratome and placed onto gelatinized slides for processing. Sections were rinsed in dH_2O, incubated in ammonium hydroxide followed by a

developing solution (Kodak Rapid Fix), and dehydrated in a graded series of EtOH solutions. Sections were then cleared with a chloroform/xylene/alcohol solution, and cover-slipped with a mounting medium (Permount, Sigma Aldrich). These procedures are detailed in several prior experiments (Bergstrom et al., 2010; Ehlinger et al., 2016), and were adapted from a previous protocol (Gibb and Kolb, 1998).

Imaging and 3D dendritic reconstruction

Golgi-stained MSNs from the dorsal striatum were visualized using brightfield microscopy (Olympus BX51) under a 60x objective connected to a Microfire CCD camera and digitally/manually reconstructed in 3D using Neurolucida (MBF Biosciences, Williston, VT, USA). All experimenters were blinded to the experimental conditions. MSNs were sampled randomly from both hemispheres and identified by soma size (~10–20 μm diameter), stellate shape (spherical dendritic radiation), the presence of three or more smooth primary dendrites and higher order dendrites covered by a high density of dendritic spines. Only fully stained MSNs with dendrites unobstructed by neighboring cells or blood vessels that could be followed from soma to terminal tip without interruption were chosen for digital reconstruction (Fig. 1). These neurons were most often located in the middle of the tissue sections. The dorsal striatum was hemisected to segregate the dorsal striatum into lateral and medial ''zones" based on the corpus callosum anatomical boundary (Fig. 1). Neurons that were located at >50 μm from the hemisection were chosen for reconstruction. A total of 222 MSNs (DMS, $n = 113$; DLS, $n = 109$) were fully reconstructed in 3D and will be submitted to Neuromorpho.org for public availability.

Quantitative morphometric analysis

Morphometrics from reconstructed MSNs were obtained using Neuroexplorer (MBF Biosciences, Williston, VT, USA). Morphometric parameters obtained included total dendritic length, total number of bifurcations, branch-order analysis (centrifugal method; total dendritic length, total number of branches, and average length as a function of branch order), total terminal endings, average distance between soma and bifurcations, average distance between soma and terminal endings, average distance between terminal endings, and volume of the dendritic field (convex hull volume and surface). Finally, the distribution of dendritic material was assessed using 3D Sholl analyses (20 μm concentric increments) with parameters of dendritic length, number of bifurcations, and intersections with Sholl radii.

For initial baseline comparisons between DMS and DLS MSNs, and interactions with pretreatment (vehicle or SCH-23390) and/or treatment (vehicle or nicotine) conditions, a mean value for each animal on each morphometric measure, based on 3–4 MSNs reconstructed per region/per animal, was used for statistical analyses ($n = 8$ animals per pretreatment-treatment group). All morphometric measures fit a normal distribution within each group as assessed by Shapiro-Wilk test. A mixed-ANOVA with the between-subject factors of pretreatment drug (vehicle or SCH-23390) and treatment drug (vehicle or nicotine) and the within-subject factors of region (DMS and DLS) and either distance from the soma (Sholl analysis) or branch-order (branch-order analysis) was conducted. Following significant interactions ($p < 0.05$), separate mixed-ANOVAs within brain region followed by Tukey's post-hoc comparisons (significance at $p < 0.05$) were conducted to determine (1) the effect of nicotine (vehicle-vehicle vs. vehicle-nicotine), (2) the effect of D1-receptor blockade on nicotine (vehicle-nicotine vs. SCH-23390-nicotine) and (3) the effect of D1-receptor blockade alone (vehicle-vehicle vs. SCH-23390-vehicle). Violation of the assumption of sphericity for repeated measures was corrected using the Greenhouse–Geisser correction for degrees of freedom (superscripted letter ''a" proceeding an F value indicates Greenhouse–Geis ser-corrected value for degrees of freedom). To further assess the distance from the soma at which dendritic remodeling occurs, comparisons between groups were made at specific radii from the soma (Sholl analysis) or branch order (branch-order analysis) using independent t tests with significance determined as $p < 0.05$ at consecutive radii or branch order (Bergstrom et al. 2010; Ehlinger et al., 2012, 2016).

To assess nicotine and D1-dependent dendritic remodeling in morphological subpopulations of MSNs, the median number of primary branches (first-order branches extending from the soma) across all pretreatment-treatment groups was obtained and reconstructed MSN's were segregated into ''large" (number of primary branches greater than 4) or ''small" (number of primary branches less than or equal to four). In total, 90 MSNs fit a classification of large (DMS, $n = 46$; DLS, $n = 44$) and 122 MSNs fit a classification of small (DMS, $n = 67$; DLS, $n = 65$). This classification system was based on data previously generated from bacterial artificial chromosome (BAC) transgenic mice with MSN sub-type specific fluorescent reporter expression (Gertler et al., 2008), as well as data showing that nicotine does not directly influence primary dendritic branches in the VS (McDonald et al., 2005; Ehlinger et al., 2016). Mixed-ANOVAs were performed as previously described, but with an additional between-group factor of MSN cell-type (large or small) followed by Tukey-Kramer post-hoc comparisons (significance at $p < 0.05$), using morphometric measures of individual cells for statistical analysis between groups.

Finally, a principal components analysis (PCA) was performed to confirm that the structural features of large and small subpopulations could be reproduced utilizing an unbiased approach (i.e. without a priori knowledge of potential MSN subpopulations). Thirteen morphological parameters that are uniquely relevant to overall dendrite morphology were obtained from NeuroExplorer for each MSN from the entire collection of reconstructed cells. These parameters were: total dendritic length, total

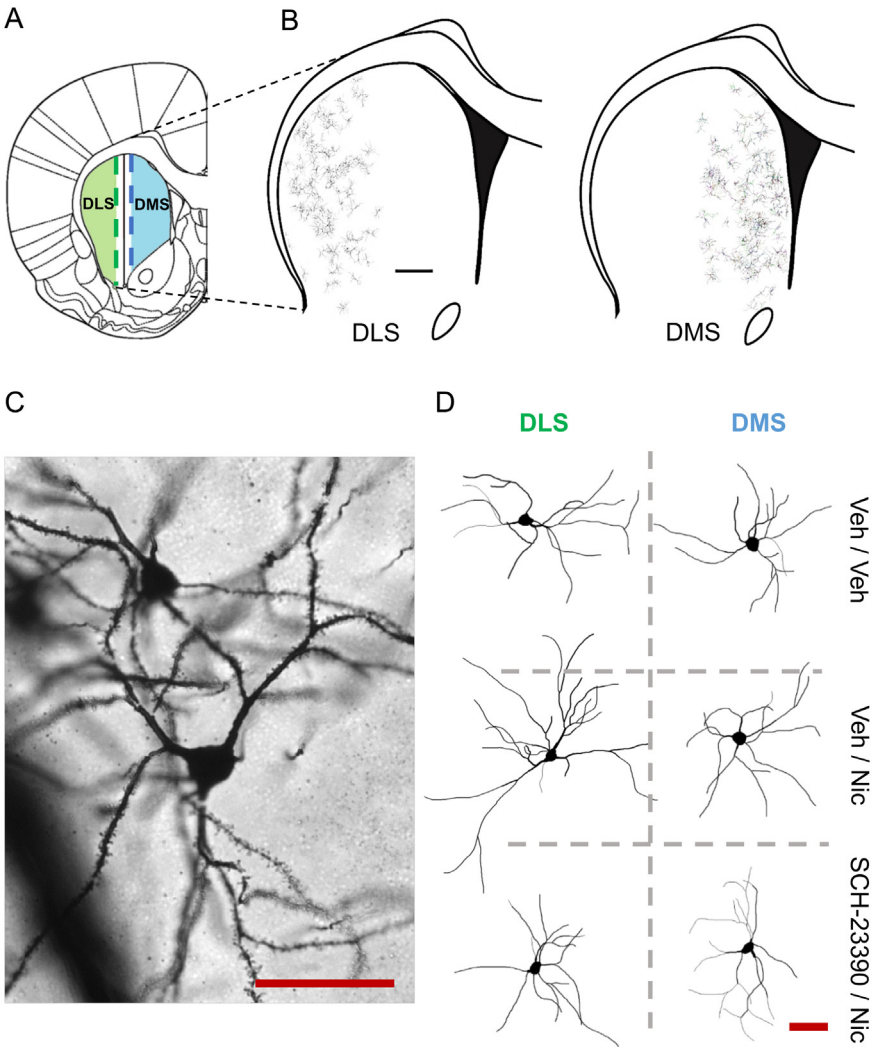

Fig. 1. Representative dorsal lateral striatum (DLS) and dorsal medial striatum (DMS) medium spiny neuron (MSN) reconstructions and micrograph. (A) Boundaries of DLS (green) and DMS (blue). (B) Maps displaying the X-Y location of all reconstructed DLS (left) and DMS (right) MSNs. Scale bar = 500 μm. (C) Micrograph of Golgi-Cox stained MSN from the DMS imaged under a 60× objective. Scale bar = 50 μm. (D) Representative MSN reconstructions. *X-axis*, dorsal striatum region. *Y-axis*, pretreatment/treatment group. Scale bar = 50 μm. (For interpretation of the references to color in this figure legend, the reader is referred to the web version of this article.)

intersections with Sholl radii, total bifurcations, total terminal endings, number of first order branches, average length of first order branches, number of late order branches (≥5th order), total length of late order branches, average branch order ($\sum$ [number of branches within each branch order × branch order] ÷ total number of branches), dendritic field volume (3D convex hull), average radial distance from soma to bifurcation, average radial distance from soma to terminal endings, and average distance between terminal endings (nearest neighbor). PCA was performed in SPSS. A covariance association matrix was obtained and assessed prior to continuing with the PCA (Bartlett's test of Sphericity, $p < 0.001$; Keyser-Meyer-Olkin MSA > 0.70). Components with eigenvalues > 1.0 were assessed and subjected to varimax rotation to obtain simple structure. The rotated correlation matrix was used to assess individual parameters with a component (factor) loading > 0.40. Component scores were obtained for every reconstructed MSN, and used to plot individual MSNs by component 1 and component 2 (see results section).

RESULTS

A quantitative morphometry of DLS and DMS MSNs

First, we assessed overall differences in dendritic morphology of MSNs between dorsal striatal regions (DLS and DMS) in vehicle treatment animals (PN63). ANOVA revealed a main effect of region on dendritic length ($F_{(1,14)} = 10.470$, $p = 0.006$), number of bifurcations ($F_{(1,14)} = 6.981$, $p = 0.019$), and intersections with sholl radii ($F_{(1,14)} = 11.296$, $p = 0.005$), indicating an overall increased size and complexity of baseline DLS MSN dendrite morphology compared to DMS MSNs. In combination with additional baseline differences in morphology described in Table 1, these results reveal a natural asymmetry in MSN dendrite morphology between the DLS and DMS.

D1-receptor-dependent nicotine-induced dendrite remodeling in DLS and DMS

To examine whether nicotine induces D1-dependent dendrite remodeling in dorsal striatum MSNs, we compared dendrite remodeling in DLS and DMS MSNs from rats exposed to chronic nicotine during adolescence, with or without co-administration of the D1-type dopamine receptor antagonist SCH-23390. For all morphological parameters measured, no differences were observed between vehicle-vehicle and SCH-23390-vehicle pretreatment-treatment groups. Therefore, representative DMS and DLS MSN reconstructions from vehicle-vehicle, vehicle-nicotine, and SCH-23390-nicotine pretreatment-treatment groups are displayed in Fig. 1. In the DLS, mixed ANOVA revealed a significant interaction between pretreatment (vehicle, SCH-23390) and treatment (vehicle, nicotine) on total dendritic length ($F_{(1,28)} = 6.389$, $p = 0.017$) and total intersections with sholl radii ($F_{(1,28)} = 6.065$, $p = 0.02$), as well as a trend toward an interaction for total number of bifurcations ($F_{(1,28)} = 2.996$, $p = 0.094$). Within saline pretreatment animals, nicotine significantly increased the total dendritic

Table 1. Morphometric parameters of control DMS and DLS MSNs

Parameter	Dorsal medial striatum $n = 58$			Dorsal lateral striatum $n = 52$		
	Average		*SEM*	*Average*		*SEM*
Soma						
Max Feret (μm)	16.58	±	0.32	15.29	±	0.40*
Min Feret (μm)	10.71	±	0.23	9.49	±	0.24*
Ratio	1.59	±	0.04	1.64	±	0.05
Dendrites						
Branch order analysis						
Total length (μm)	1199.02	±	55.74	1413.04	±	64.18*
1st order	118.82	±	12.33	128.25	±	14.56
2nd order	327.40	±	21.33	311.20	±	20.66
≥5th order	129.97	±	24.11	269.73	±	42.56*
Total branches (#)	25.53	±	0.99	29.38	±	1.25*
1st order	4.57	±	0.17	4.42	±	0.16
2nd order	7.22	±	0.30	6.92	±	0.29
≥5th order	2.38	±	0.41	4.81	±	0.72*
Average length (μm)						
1st order	25.11	±	2.34	27.69	±	2.85
2nd order	44.53	±	1.89	44.00	±	2.10
≥5th order	28.55	±	4.33	37.00	±	4.10
Sholl intersections (#)	49.41	±	2.38	58.56	±	2.67*
Bifurcations (#)	10.53	±	0.48	12.50	±	0.62*
Terminal endings (#)	15.05	±	0.52	16.90	±	0.64*
Soma to bifurcation distance (μm)	29.15	±	1.52	34.64	±	1.44*
Soma to terminal distance (μm)	101.57	±	2.59	111.06	±	2.73*
Distance between terminal ends (μm)	37.22	±	1.08	38.94	±	1.14
Convex hull volume (μm^3)	447211.6	±	55458.3	616047.4	±	73520.35^
Convex hull surface (μm^2)	63485.57	±	3259.98	79687.17	±	4438.06*

DMS vs DLS, *$p < 0.05$; ^$p < 0.10$.

length ($t[14] = 2.424$, $p = 0.030$) and number of intersections with sholl radii ($t[14] = 2.935$, $p = 0.011$) of DLS MSNs (Tukey-*HSD* < 0.05). Statistical analysis also revealed a trend toward a nicotine-induced increase in total number of bifurcations ($t[14] = 1.903$, $p = 0.078$; Tukey-*HSD* > 0.05). These alterations were most prominent between 60 to 100 μm from the soma. SCH-23390 pretreatment completely blocked these nicotine-induced increases in total dendritic length ($t[14] = 2.632$, $p = 0.020$) and intersections with sholl radii ($t[14] = 2.781$, $p = 0.015$; Tukey-*HSD* < 0.05), and partially decreased the number of bifurcations ($t[14] = 2.446$, $p = 0.028$; Tukey-*HSD* > 0.05), of DLS MSNs (Fig. 2). In contrast, no main effects or interactions between pretreatment and treatment on dendritic length, intersections with sholl radii, and number of bifurcations were observed in the DMS. Collectively, these results suggest that nicotine exposure selectively remodels dendrites in the DLS, and that activity at D1-type dopamine receptors during the time-course of nicotine exposure is required for nicotine-induced DLS dendritic remodeling. These results are strikingly similar to those reported previously for ventral striatum (VS) MSNs (Ehlinger et al., 2016).

Anatomical segregation and morphological characterization of dorsal striatal MSNs

MSNs can be broadly classified into D1- and D2-type dopamine receptor expressing cells (Gerfen et al., 1990) corresponding to the direct and indirect striatal pathways, respectively, with only a small population of MSNs expressing both receptor-types (Perreault et al., 2011; Gagnon et al., 2017). Therefore, it is possible that the D1-dependent nicotine-induced restructuring of dendrite morphology that we observe is subpopulation specific. However, D1- and D2- type MSNs are randomly distributed throughout the striatum (Gangarossa et al., 2013) and co-immunolabeling for these dopamine receptor subtypes is not possible in rat Golgi stained tissue, making a detailed cell-type specific classification of MSNs a technical limitation. However, several reports in transgenic mice utilizing D1- and D2-receptor-dependent fluorescent reporters have shown that these MSN subtypes display unique dendritic morphologies in which D1-receptor expressing MSNs contain a larger volume of the dendritic arbor and/or a greater number of primary dendrites extending from the cell body compared to D2-expressing MSNs (Gertler et al., 2008; Gagnon et al., 2017). Whether similar morphological features of dorsal

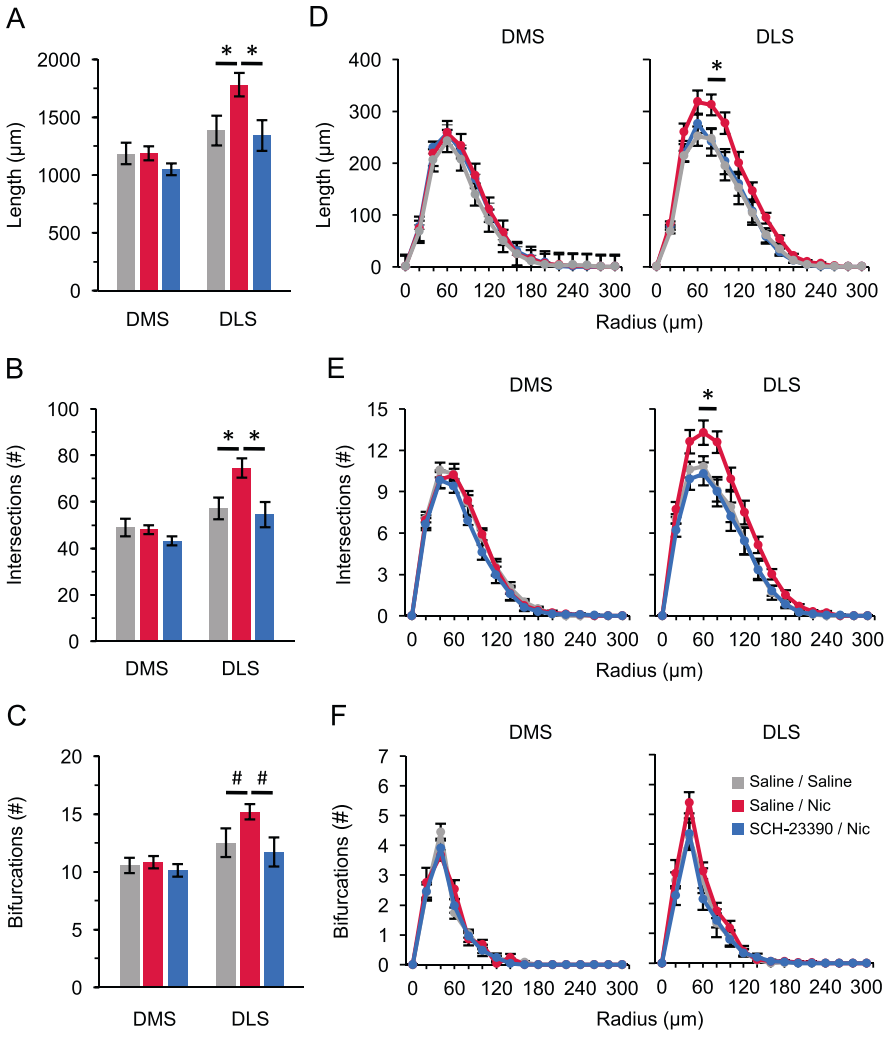

Fig. 2. Influence of nicotine and co-administered D1DR antagonist SCH-23390 on DLS and DMS medium spiny neuron (MSN) dendrite morphology. No effects of SCH alone were found in any analyses. For clarity, data from SCH-Veh treatment animals are not presented. (A–C) Values represent group mean ± SEM for each total morphological measure. $^{*}t$-test and Tukey-HSD $p < 0.05$. $^{\#}t$-test or Tukey-HSD $p < 0.10$. (D–F) Sholl analyses (20 μm increments). Each point represents group mean ± SEM. $^{*}t$-test for vehicle-vehicle compared to both vehicle-nicotine and SCH23390-nicotine $p < 0.05$ at consecutive Sholl radii.

striatal MSNs translate to the rat has yet to be explored, and classification of MSNs into subpopulations based on distinct morphological features could reveal whether nicotine-induced dendritic remodeling and blockade via SCH-23390 is specific for dorsal striatal MSN subpopulation.

To explore this possibility, we segregated reconstructed MSNs from both the DLS and DMS using a median-split on the number of primary branches into "large" (>4 primary dendrites) and "small" (3–4 primary dendrites) cell types (Fig. 3). This parameter was chosen based on (1) previous reports in mouse models suggesting that this parameter defines D1 and D2 expressing MSN subtypes (Gertler et al., 2008), (2) the hypothesis that a similar criteria would translate to rat Golgi-Cox stained tissue, and (3) data obtained from both the present study (Fig. 2) and previous work (McDonald et al., 2005, 2007; Ehlinger et al., 2016) confirming that nicotine does not influence primary dendrite number or morphology, eliminating the potential confound of subpopulation segregation based on a morphological parameter that is influenced by nicotine exposure.

First, we assessed baseline differences between large and small MSN subpopulations within the DMS and DLS of vehicle treatment animals. ANOVA revealed no main effects nor interactions between cell type or region with pretreatment (vehicle or SCH-23390) on any morphological measure examined (pretreatment x cell type x region on total bifurcations, $p = 0.178$; on total length, $p = 0.308$), therefore, further analysis of baseline differences in dendrite morphology between large and small MSNs included cells from both vehicle and SCH-23390 pretreatment (saline treatment) animals. ANOVA revealed a significant main effect of both region ($F_{(1,102)} = 5.901$, $p = 0.017$) and cell-type ($F_{(1,102)} = 5.675$, $p = 0.019$) on total dendritic length, yet no effect on the total number of bifurcations. However, a significant interaction between branch order and cell-type was observed on total dendritic length ($F_{a(3.7,375.3)} = 7.506$, $p < 0.001$), number of dendritic branches ($F_{a(3.4,342.7)} = 13.431$, $p < 0.001$), and average branch length ($F_{a(4.4,448.6)} = 4.427$, $p = 0.001$). Specifically, while large MSNs have a higher total number, length, and average length of primary and secondary dendritic branches, they also display a smaller number, total length, and average length of 5th and 6th order dendritic branches (Fig. 3, Table 2). Collectively, these results suggest that despite an overall greater total amount of dendritic material in large MSNs as compared to small MSNs, their distal dendritic arbors are initially less complex.

To further confirm this morphological classification of MSN subpopulations, we asked whether an unbiased (i.e. without a priori knowledge of potential subpopulations) statistical method would reproduce similar morphological features that could define MSN subpopulations. To this end, 13 morphological parameters that are representative of the overall size and shape of the dendritic arbor were loaded into a principal components analysis (PCA-varimax rotation) and was applied to the entire collection of reconstructed MSN (DMS and DLS; vehicle, nicotine, and SCH23390

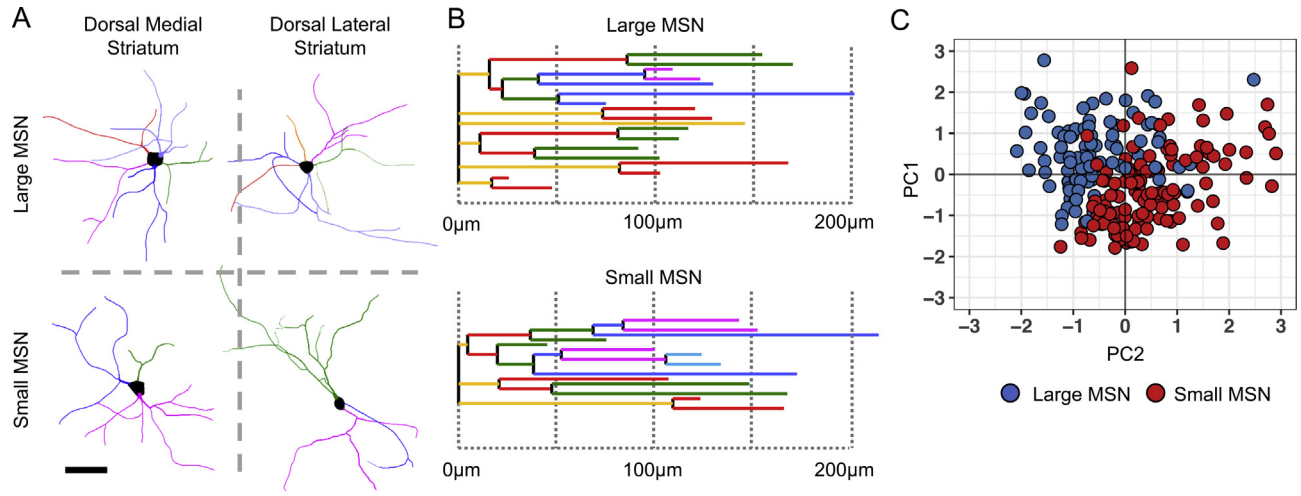

Fig. 3. Segregation of DLS and DMS medium spiny neurons (MSNs) into "large" and "small" subpopulations. (A) Representative (±SEM) MSN reconstructions from vehicle treatment groups. Each primary dendrite and its corresponding dendritic tree is displayed in a different color to visualize the number of primary dendrites in large vs. small MSNs. *X-axis*, dorsal striatum region. *Y-axis*, cell-type. Scale bar = 50 μm. (B) Representative (±SEM) dendrograms of large and small MSNs from vehicle treatment groups. Dendrogram is colored by branch order. Large MSNs are characterized by having >4 primary dendrites and a fewer number of 5th and 6th order branches, while small MSNs are characterized by having 3–4 primary dendrites and a greater number of 5th and 6th order branches. Additional morphometric comparisons between the MSN subpopulations are displayed in Table 2. (C) Plot comparing the entire collection of $N = 222$ reconstructed large (blue) and small (red) MSNs across principal components (PC) 1 and 2, as defined in Table 3. (For interpretation of the references to color in this figure legend, the reader is referred to the web version of this article.)

pretreatment/treatment groups). The PCA extracted three unique components (eigenvalues >1.0) accounting for approximately 80% of the variance (Table 3). As expected, parameters loading on to component 1 (36.5% of variance) reflect the variation in the total amount of dendritic material, including all parameters observed to be directly enhanced by nicotine exposure as well as the total number of primary dendrites. Most interestingly, parameters loading on to component 2 (26.7% of variance) indicated an anticorrelation between the total number of primary branches and both the quantity and total length of late order branches. This finding illustrates that an accurate description of variability in morphological features is revealed when MSNs are segregated into large and small subpopulations based solely on the number of primary dendrites (Fig. 3). Finally, morphological parameters loading in component 3 (17% of variance) appear to reflect the "spread" of the dendritic arbor. Collectively, these results confirm that the number of primary dendrites present on MSNs represents a unique source of variance in dorsal striatal MSN morphology that is independent from variation in total dendritic material, further supporting the segregation of MSNs into large and small subpopulations based on the number of primary branches.

D1-dependent nicotine-induced dendrite remodeling is DLS subpopulation specific

Finally, we hypothesized that nicotine-induced dendritic remodeling would be selectively enhanced in the large MSN subpopulation, and that this class of MSN would be uniquely impacted by SCH-23390 co-administration during nicotine exposure. For large MSNs, a significant interaction between pretreatment (vehicle, SCH-23390) and treatment (vehicle, nicotine) was observed in the DLS on the total number of bifurcations ($F_{(1,40)} = 7.763$, $p = 0.008$) and a trend for total length ($F_{(1,40)} = 3.052$, $p = 0.09$), as well as a significant interaction between branch order, pretreatment, and treatment on the number of dendritic branches ($F_{a(3.2,136.3)} = 3.194$, $p = 0.021$). For large MSNs of the DLS, nicotine significantly increased the total number of bifurcations ($t[24] = 2.820$, $p = 0.009$) and total dendritic length ($t[24] = 2.596$, $p = 0.016$) (Tukey-*HSD* < 0.05). SCH-23390 pretreatment completely blocked the nicotine-induced increase in the total number of bifurcations, but not total dendritic length, of large MSNs within the DLS ($t[17] = 2.501$, $p = 0.021$; Tukey-*HSD* < 0.05). These alterations in dendritic morphology of large DLS MSNs were most prominent in the distal dendritic arbor (5th and 6th order branches) (Fig. 4). In contrast, no main effects or interactions between pretreatment, treatment, and branch order were observed in DLS small MSNs or in DMS large and small MSNs on any morphological measure examined (Tukey-*HSD* > 0.05). Collectively, these results suggest that nicotine selectively induces dendritic remodeling in a morphological subpopulation of DLS MSNs (large subtype) that are characterized by their higher number of primary dendrites, while leaving small MSNs of the DLS and *all* MSNs of the DMS unaffected. Furthermore, co-administration of the D1-type dopamine receptor antagonist SCH-23390 blocks nicotine-induced dendritic remodeling in large DLS MSNs, revealing that the observed subpopulation specific effects of nicotine exposure during adolescence are dependent on dopamine signaling at D1 receptors during the time-course of nicotine exposure.

Table 2. Morphometric parameters of control large and small MSNs within DMS and DLS

Parameter		Dorsal medial striatum				Dorsal lateral striatum			
		Large cells $n = 27$		Small cells $n = 31$		Large cells $n = 22$		Small cells $n = 30$	
		Average	*SEM*	*Average*	*SEM*	*Average*	*SEM*	*Average*	*SEM*
Soma									
	Max Feret (μm)	16.46	± 0.47	16.68	± 0.45	15.42	± 0.54	15.19	± 0.58
	Min Feret (μm)	11.31	± 0.30	10.19	± 0.32*	9.66	± 0.33	9.36	± 0.35
	Ratio	1.47	± 0.05	1.69	± 0.07*	1.62	± 0.06	1.66	± 0.07
Dendrites									
	Branch order analysis								
	Total length (μm)	1305.96	± 76.26	1105.84	± 77.68^	1542.25	± 85.02	1318.28	± 89.36^
	1st order	149.74	± 18.68	91.89	± 14.99*	187.42	± 23.50	84.85	± 14.12*
	2nd order	423.89	± 33.13	243.35	± 16.82*	388.47	± 35.67	254.54	± 19.09*
	≥5th order	66.29	± 20.80	185.43	± 38.97*	189.67	± 52.56	328.44	± 61.43^
	Total branches (#)	27.90	± 1.34	24.10	± 1.40	30.77	± 1.62	28.37	± 1.81
	1st order	5.67	± 0.18	3.61	± 0.09*	5.50	± 0.17	3.63	± 0.09*
	2nd order	8.48	± 0.46	6.13	± 0.28*	7.91	± 0.48	6.20	± 0.29*
	≥5th order	1.19	± 0.34	3.42	± 0.65*	3.27	± 0.82	5.93	± 1.06^
	Average length (μm)								
	1st order	25.66	± 2.74	24.63	± 3.70	33.62	± 4.07	23.34	± 3.8^
	2nd order	49.96	± 2.46	39.80	± 2.56*	48.24	± 3.35	40.89	± 2.58^
	≥5th order	19.72	± 5.66	36.24	± 6.19*	32.33	± 6.65	40.42	± 5.18
	Sholl intersections (#)	54.07	± 3.35	45.35	± 3.25^	63.91	± 3.53	54.63	± 3.71^
	Bifurcations (#)	10.85	± 0.68	10.26	± 0.69	12.64	± 0.81	12.40	± 0.90
	Terminal endings (#)	16.43	± 0.69	13.85	± 0.71*	18.14	± 0.82	16.00	± 0.92*
	Soma to bifurcation distance (μm)	26.13	± 1.81	31.77	± 2.3^	35.05	± 2.51	34.35	± 1.72
	Soma to terminal distance (μm)	97.94	± 3.10	104.72	± 3.98	111.53	± 3.82	110.71	± 3.86
	Distance between terminal ends (μm)	34.74	± 1.23	39.37	± 1.64*	38.41	± 1.50	39.34	± 1.66
	Convex hull volume (μm^3)	462621.6	± 87102.2	433790.0	± 72067.0	701301.6	± 93710.0	553527.6	± 107213.7
	Convex hull surface (μm^2)	63963.62	± 4339.33	63069.20	± 4853.16	87414.20	± 6507.76	74020.68	± 5910.42

Large vs small within DMS or DLS, *$p < 0.05$; ^$p < 0.10$.

DISCUSSION

Neuroplasticity in the striatum underlies nicotine reinforcement and the progression to addiction (Everitt and Robbins, 2005). Dendritic remodeling is a fundamental form of neuroplasticity commonly observed after chronic exposure to all drugs of abuse (Russo et al., 2010), including nicotine (Smith et al., 2015b). While the ventral striatum has consistently been associated with persisting changes in the morphology of dendrites after nicotine (Brown and Kolb, 2001; McDonald et al., 2005, 2007; Ehlinger et al., 2016), in this study we asked whether nicotine similarly remodels dendrites in the dorsal striatum. First, this study revealed a pre-existing asymmetry of MSN dendritic complexity in which DLS MSNs exhibit more dendritic complexity compared to DMS MSNs. Second, chronic nicotine induced a robust, selective, and persistent increase in the size and complexity of MSNs of the DLS, but not DMS. Third, a unique morphological feature of dorsal striatal MSNs was revealed in which the number of primary dendrites was negatively correlated with the number of distal dendrites, and nicotine selectively increased the complexity of the distal dendritic arbor in a MSN subpopulation defined by a higher number of primary dendrites. Finally, structural plasticity of this DLS subpopulation was totally reversed in the presence of the selective D1-receptor antagonist SCH-23390 during the time-course of nicotine exposure.

Asymmetry of MSN dendritic complexity across the mediolateral axis of the dorsal striatum

GABAergic projection medium-spiny neurons (MSN) represent 95% of neural cell-types in the striatum (Gerfen and Wilson, 1996; Gertler et al., 2008). An unexpected finding in the present experiment was a robust, naturally existing asymmetry in the size and complexity of MSNs across the DLS and DMS. Specifically, DLS MSN dendritic arbors were found to be larger overall (17.8% difference) and more complex, based on nodes and bifurcation number, compared to MSN dendritic arbors found in the DMS (Table 1). Even within morphologically defined MSN subpopulations, both large and small MSNs were found to be larger in the DLS than in the DMS (Table 2). To our knowledge, this is the first evidence suggesting a naturally existing asymmetry of MSN dendrite morphometry across the mediolateral axis of the DS. This finding has important implications for the normative subnetwork functionality of the striatum, as dendritic morphometry can shape information processing of neural networks (Chklovskii et al., 2004; Stuart et al., 2016). Naturally greater elaboration and complexity of MSN dendritic

Table 3. PCA rotated components matrix

Parameter	Component		
	PC1	PC2	PC3
Total length	**0.94**		
Total intersections	**0.93**		
# Terminal ends	**0.88**		
Total bifurcations	0.79	0.51	
Convex hull volume	0.72		0.43
Avg. branch order		**0.90**	
# Late order branches		**0.86**	
Total length – late order branches		**0.82**	
# First order branches	**0.58**	**−0.64**	
Terminals – nearest neighbor			**0.83**
Terminals – distance from soma	0.52		0.72
Average length first order branches			**0.61**
Bifurcations – distance from soma		0.40	0.51

Only factor loadings ≥0.40 are displayed for clarity.
Parameters uniquely or differentially loading within components are in bold text.

arbors may confer differential information-processing capability in the DLS and DMS, including (but not limited to) habitual responsivity and addiction related behavior.

The DLS, habits, and nicotine addiction

Dendritic remodeling is a fundamental form of circuit plasticity associated with changes in synaptic and functional network connectivity (Stepanyants and Chklovskii, 2005), and multiple drugs of abuse have been found to produce lasting and preferential changes on neuronal structure in the dorsal lateral striatum. Methamphetamine produces a long-lasting (3 months) increase in the density of dendritic spines in the DLS, but a decrease in spine density in the DMS (Jedynak et al., 2007). Alcohol increased the length of dendrites in mouse DLS (DePoy et al., 2013) and increased the density of spines in the primate putamen (DLS analog), but not caudate (DMS analog) nucleus (Carlson et al., 2011). Chronic stress has also been found to increase the complexity of dendrites in the DLS, but not DMS (Taylor et al., 2014), a finding that is of particular interest in view of the role of stress in promoting drug-taking and habit formation (Schwabe et al., 2011). The current data support and extend these findings by demonstrating a lasting form of dendritic restructuring that is selective for the DLS following chronic nicotine exposure during adolescence. Considering the role of the DLS in the expression of habitual behavior (Yin and Knowlton, 2006; Graybiel and Grafton, 2015), these data support an addiction model whereby long-lasting modifications in dendritic structure in the DLS may promote addictive behavior. Furthermore, given that addiction is defined by persisting changes in mesolimbic neuronal circuits over protracted time frames (O'Brien and McLellan, 1996), long-lasting structural alterations in DLS dendrites may represent a "nicotine engram" that underlies and contributes to an increased propensity for relapse (Hsiang et al., 2014).

Despite the absence of nicotine-induced structural alterations in the DMS in the present study, DMS neuroplasticity has been observed following exposure to several classes of addictive drugs, including structural and functional changes after alcohol (Wang et al., 2015; Cheng et al., 2016), cocaine (Gourley et al., 2013), methamphetamine (Furlong et al., 2015) and nicotine (Clemens et al., 2014). However, most of these studies assayed neuroplasticity in the DMS at relatively short time frames following cessation of drug exposure. In a between-subject experimental design, we have previously demonstrated a lasting form of dendritic remodeling in the ventral striatum that was present both immediately following the cessation of chronic nicotine and that persisted through an extended abstinence period (21 days) (Ehlinger et al., 2016), suggesting neuroadaptations in the VS emerge rapidly, likely during drug administration. It is possible that dendritic remodeling in the DMS may have emerged rapidly, but then returned to a "baseline" morphology over the course of protracted withdrawal (21-days). This model would sharply contrast with the present data for the DLS, indicating that neuroadaptations in the DLS emerged either during nicotine administration, or over the course of protracted withdrawal, and *persisted* for at least 21 days following the nicotine regimen. The potential for contrasting temporal dynamics of persisting nicotine-induced dendritic plasticity in the DLS and DMS would parallel evidence for contrasting functionality of these regions in reinforcement learning and memory (Balleine and O'Doherty, 2010). Specifically, it can be speculated that habit performance requires a more persisting form of neuroplasticity, while flexible, goal-directed learning requires a less permanent form of plasticity for the establishment of action selection sequences.

The adolescent brain responds differently to all drugs of abuse, including nicotine (Spear, 2016). Here, nicotine was administered during adolescence (PN28-42) and lasting changes in DLS dendrite structure were observed in early adulthood (PN63). How the observed pattern of morphological changes extend to the adult brain is an open question. Nicotine exposure during adolescence has been shown to enhance structural plasticity in the VS when directly compared to adult exposure (McDonald et al., 2007). It might be expected that adult exposure would produce a similar, albeit smaller, pattern of structural changes in DLS MSNs. There are also data in adolescent humans (12–16 years old) showing a reduction in gray matter in the putamen (DLS analog) compared with adults (Sowell et al., 1999). Consistent with the viewpoint that the unique development profile of the adolescent brain may confer differential vulnerability to drug-induced plasticity as compared with the adult brain (Smith et al., 2015b), ongoing neurodevelopment of the adolescent DLS may render it uniquely susceptible to persisting nicotine-induced plasticity.

Persisting effects of chronic nicotine in a putative DLS direct pathway

Emerging evidence indicates that drugs of abuse differentially modify the structure and function of the direct (D1-type) and indirect (D2-type) striatal pathways (Lobo and Nestler, 2011; Bock et al., 2013; Wang et al., 2015). Using BAC-transgenic mice, D1-type (direct pathway) striatal MSNs have been found to possess more primary dendrites and an overall great amount of dendritic material relative to D2-type (indirect-pathway) striatal

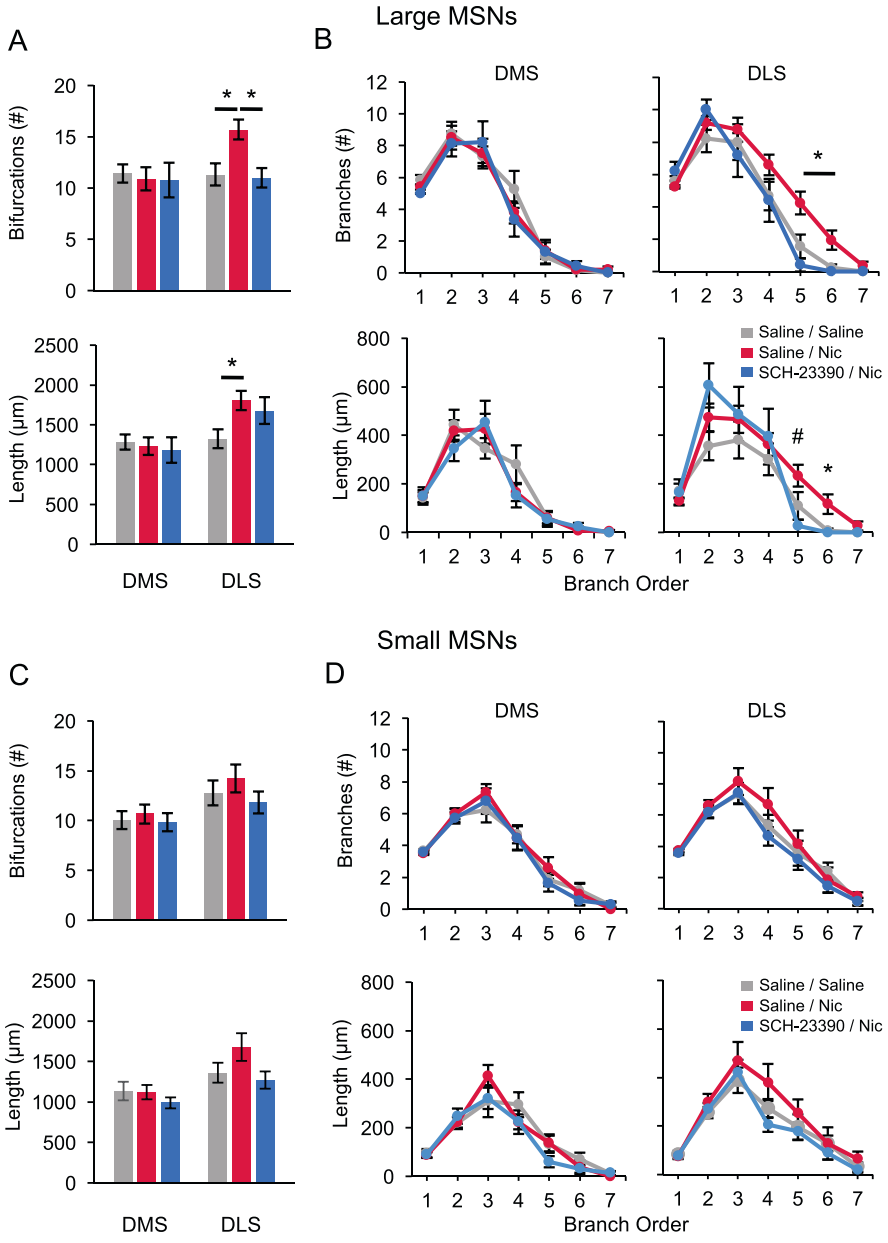

Fig. 4. Influence of nicotine and co-administered D1DR antagonist SCH-23390 on large and small medium spiny neurons (MSNs) from the DLS and DMS. No effects of SCH alone were found in any analyses. For clarity, data from SCH-Veh treatment animals are not presented. (A, B). Values represent mean of all cells ± SEM for each total morphological measure. $^{*}t$-test and Tukey-HSD $p < 0.05$. (C, D) Branch-order analyses (centrifugal method: 1 = primary dendrite). Each point represents mean of all cells ± SEM. $^{*}t$-test for vehicle-vehicle compared to both vehicle-nicotine and SCH23390-nicotine $p < 0.05$. $^{\#}p < 0.10$.

MSNs (Gertler et al., 2008; Gagnon et al., 2017). Here, not only do we report that chronic nicotine exposure during adolescence preferentially increases the complexity of DLS MSNs that display more primary dendrites and a larger overall dendritic arbor, but that D1 antagonist co-administration completely reversed these effects. Therefore, we speculate that the present data reflect nicotine-induced restructuring preferentially in, or in a larger proportion of, direct pathway MSNs. This conclusion is tentative as it is not possible to neurochemically profile these morphologically defined subtypes in Golgi-stained tissue. Furthermore, there is no firm "cut-off" for the number of primary dendrites that designates D1 from D2-type MSNs; it is more likely that D1- and D2-type MSNs exist along a morphological continuum. Nevertheless, the present study reveals that nicotine is selective for a morphological subtype of MSN expressing a higher number of primary dendrites, selectively within the DLS, and that co-administration of a D1 antagonist prevented the expansion of dendritic complexity within this subpopulation. The application and further development of cell-type-specific technologies that can be used in the rat and are capable of illuminating the entire dendritic arbor while maintaining both sparse labeling and neurochemical integrity (e.g. viral-mediated gene transfer, fluorescent reporters, DiOlistic labeling), will be required to confirm the phenotype of these morphologically defined subtypes (Gertler et al., 2008; Gagnon et al., 2017).

Several factors could account for cell-type specificity of nicotine-induced dendritic remodeling revealed in the present study. First, unique molecular characteristics of dopamine D1 receptor (D1R) vs. D2R signaling would certainly be expected to differentially influence structural plasticity between MSN subtypes. Most prominently, D1Rs are positively coupled to the cAMP-PKA pathway while D2Rs are negatively coupled to the cAMP-PKA pathway (Gerfen and Surmeier, 2011; Lobo and Nestler, 2011), leading to differences in intracellular signaling that can profoundly influence the pattern of gene transcription responsible for structural plasticity within cell-types (Nestler, 2004), as evidenced by enhanced and long-lasting delta-FosB expression preferentially in D1 MSNs following cocaine exposure (Lobo et al., 2013). Second, the precise pharmacological mechanisms by which different psychostimulants influence dopamine transmission to the striatum could lead to different patterns of structural plasticity across MSN subtypes. For example, cocaine has been shown to influence structural remodeling in both D1 and D2 cell types (Li et al., 2012). Importantly, while cocaine acts directly on dopaminergic terminals in the striatum by blocking the dopamine active transporter, nicotine enhances dopamine release

in the striatum via action on nicotinic acetylcholine receptors that are located on both midbrain dopaminergic cell bodies (Picciotto et al., 1998) and axons (Rice and Cragg, 2004; Zhang and Sulzer, 2004), acting to preferentially increase phasic dopaminergic neuron activity and enhance striatal dopamine release. Although single dopaminergic axons are extremely large and are likely to innervate both MSN subpopulations within a given striatal region, an intriguing possibility is that the altered activity pattern of midbrain dopamine neurons during nicotine exposure preferentially influences D1 vs D2 MSNs. In fact, the projections and activity patterns of non-dopaminergic neurotransmitter systems could differentially influence the neuroplastic effects of dopamine on striatal MSN subtypes. For example, glutamate-induced excitatory post-synaptic currents (EPSCs) are differentially modulated by dopamine in MSNs (André et al., 2010). Heinsbroek and colleagues (2017) revealed that GABAergic long-term depression (LTD), a form of synaptic plasticity, is maintained for at least 28-days only on D1R expressing MSNs and is disrupted on D2R expressing MSNs following cocaine exposure (Heinsbroek et al., 2017). Most recently, it was shown that while the activity of GABAergic interneurons within the DLS is initially strengthened during reinforcement learning it diminishes with increasing experience (Lee et al., 2017), suggesting additional mechanisms for both regional and cell-type specific effects of nicotine. Therefore, differences in dopaminergic, glutamatergic excitatory, and GABAergic inhibitory control of direct vs. indirect pathway MSNs are likely influences on the pattern of D1R-dependent nicotine-induced dendrite remodeling revealed in the present study.

Morphological properties of MSNs

A segregation of dorsal striatal MSNs into morphological subpopulations revealed a naturally existing negative correlation between primary dendrites and higher order branching. That is, MSNs with more proximal (primary) branches had fewer distal branches and vice versa (Fig. 3). It was also shown that nicotine selectivity increases branching at the distal portion of the dendritic tree only in MSNs with relatively more primary dendrites. One hypothesis for a selective effect of nicotine is that MSNs with relatively few distal branches possess an increased capacity for plasticity, or alternatively, are more *vulnerable* to nicotine-induced plasticity. This possibility will require an *in vivo* imaging approach to test directly. Another interesting possibility is that nicotine might have produced a new morphological subtype that is distinct from both large and small MSN subpopulations and defined as cells with both a higher number of primary dendrites and more complex branching of the distal arbor. How these morphological changes specifically influence both large-scale network processing (e.g. corticolimbic circuitry) and/or the intrinsic microanatomy (i.e. interneuron connectivity) of the striatal system are important directions for future research.

CONCLUSIONS

More people in the United States are addicted to nicotine than any other abused drug (CDC, 2015). The present study provides evidence for a persistent, regionally selective, cell-type specific, and D1-dependent form of structural plasticity in the dorsal striatum in response to chronic nicotine. This research highlights the complex and substantial impact of nicotine on the developing adolescent brain, and adds to a growing list of corticolimbic brain regions and cell-types exhibiting a lasting, selective form of structural remodeling after nicotine that now includes the ventral striatum (Brown and Kolb, 2001; McDonald et al., 2005, 2007; Ehlinger et al., 2016), basolateral amygdala (Bergstrom et al., 2010), insular cortex (Ehlinger et al., 2012), prefrontal cortex (Bergstrom et al., 2008), hippocampus (Holliday et al., 2016) and bed nucleus of the stria terminalis (Smith et al., 2015a). Considering the critical role for the dorsal striatum in instrumental learning and the expression of habitual behavior, lasting changes in the dendritic architecture of the dorsal striatum represent an important network node for studying nicotine effects on the developing adolescent brain.

FUNDING

The Virginia Tobacco Settlement Foundation (VTSF).

Acknowledgment—The authors thank Savannah Kandigian for assistance with Fig. 1.

REFERENCES

André VM, Cepeda C, Cummings DM, Jocoy EL, Fisher YE, William Yang X, Levine MS (2010) Dopamine modulation of excitatory currents in the striatum is dictated by the expression of D1 or D2 receptors and modified by endocannabinoids. Eur J Neurosci 31:14–28.

Balleine BW, O'Doherty JP (2010) Human and rodent homologies in action control: corticostriatal determinants of goal-directed and habitual action. Neuropsychopharmacology 35:48–69.

Balleine BW, Delgado MR, Hikosaka O (2007) The role of the dorsal striatum in reward and decision-making. J Neurosci 27:8161–8165.

Belin D, Jonkman S, Dickinson A, Robbins TW, Everitt BJ (2009) Parallel and interactive learning processes within the basal ganglia: relevance for the understanding of addiction. Behav Brain Res 199:89–102.

Bergstrom HC, McDonald CG, French HT, Smith RF (2008) Continuous nicotine administration produces selective, age-dependent structural alteration of pyramidal neurons from prelimbic cortex. Synapse 62:31–39.

Bergstrom HC, Smith RF, Mollinedo NS, McDonald CG (2010) Chronic nicotine exposure produces lateralized, age-dependent dendritic remodeling in the rodent basolateral amygdala. Synapse 64:754–764.

Bock R, Shin JH, Kaplan AR, Dobi A, Markey E, Kramer PF, Gremel CM, Christensen CH, Adrover MF, Alvarez VA (2013) Strengthening the accumbal indirect pathway promotes resilience to compulsive cocaine use. Nat Neurosci 16:632–638.

Brown RW, Kolb B (2001) Nicotine sensitization increases dendritic length and spine density in the nucleus accumbens and cingulate cortex. Brain Res 899:94–100.

Carlson VCC, Seabold GK, Helms CM, Garg N, Odagiri M, Rau AR, Daunais J, Alvarez VA, Lovinger DM, Grant KA (2011) Synaptic and morphological neuroadaptations in the putamen associated with long-term, relapsing alcohol drinking in primates. Neuropsychopharmacology 36:2513–2528.
CDC (2015) Qutting Smoking. 2016.
Cheng Y, Huang CC, Ma T, Wei X, Wang X, Lu J, Wang J (2016) Distinct Synaptic Strengthening of the Striatal Direct and Indirect Pathways Drives Alcohol Consumption. Biol Psychiatry.
Chklovskii DB, Mel B, Svoboda K (2004) Cortical rewiring and information storage. Nature 431:782–788.
Clemens KJ, Castino MR, Cornish JL, Goodchild AK, Holmes NM (2014) Behavioral and neural substrates of habit formation in rats intravenously self-administering nicotine. Neuropsychopharmacology 39:2584–2593.
Corbit LH, Nie H, Janak PH (2012) Habitual alcohol seeking: time course and the contribution of subregions of the dorsal striatum. Biol Psychiatry 72:389–395.
DePoy L, Daut R, Brigman JL, MacPherson K, Crowley N, Gunduz-Cinar O, Pickens CL, Cinar R, Saksida LM, Kunos G, Lovinger DM, Bussey TJ, Camp MC, Holmes A (2013) Chronic alcohol produces neuroadaptations to prime dorsal striatal learning. Proc Natl Acad Sci U S A 110:14783–14788.
Ehlinger DG, Bergstrom HC, McDonald CG, Smith RF (2012) Nicotine-induced dendritic remodeling in the insular cortex. Neurosci Lett 516:89–93.
Ehlinger D, Bergstrom H, Burke J, Fernandez G, McDonald C, Smith R (2016) Adolescent nicotine-induced dendrite remodeling in the nucleus accumbens is rapid, persistent, and D1-dopamine receptor dependent. Brain Struct Funct 221:133–145.
Everitt BJ, Robbins TW (2005) Neural systems of reinforcement for drug addiction: from actions to habits to compulsion. Nat Neurosci 8:1481–1489.
Furlong TM, Supit AS, Corbit LH, Killcross S, Balleine BW (2015) Pulling habits out of rats: adenosine 2A receptor antagonism in dorsomedial striatum rescues meth-amphetamine-induced deficits in goal-directed action. Addict Biol.
Gagnon D, Petryszyn S, Sanchez MG, Bories C, Beaulieu JM, De Koninck Y, Parent A, Parent M (2017) Striatal neurons expressing D1 and D2 receptors are morphologically distinct and differently affected by dopamine denervation in mice. Sci Rep 7:41432.
Gangarossa G, Espallergues J, Mailly P, De Bundel D, De Kerchove D, Hervé D, Girault J, Valjent E, Krieger P (2013) Spatial distribution of D1R-and D2R-expressing medium-sized spiny neurons differs along the rostro-caudal axis of the mouse dorsal striatum. Front Neural Circuits 7:124.
Gerfen CR, Surmeier DJ (2011) Modulation of striatal projection systems by dopamine. Annu Rev Neurosci 34:441–466.
Gerfen CR, Wilson CJ (1996) The basal ganglia. Handbook Chem Neuroanat 12:371–468.
Gerfen CR, Engber TM, Mahan LC, Susel Z, Chase TN, Monsma Jr FJ, Sibley DR (1990) D1 and D2 dopamine receptor-regulated gene expression of striatonigral and striatopallidal neurons. Science 250:1429–1432.
Gertler TS, Chan CS, Surmeier DJ (2008) Dichotomous anatomical properties of adult striatal medium spiny neurons. J Neurosci 28:10814–10824.
Gibb R, Kolb B (1998) A method for vibratome sectioning of Golgi-Cox stained whole rat brain. J Neurosci Methods 79:1–4.
Gourley SL, Olevska A, Gordon J, Taylor JR (2013) Cytoskeletal determinants of stimulus-response habits. J Neurosci 33:11811–11816.
Graybiel AM (2000) The basal ganglia. Curr Biol 10:R509–R511.
Graybiel AM, Grafton ST (2015) The striatum: where skills and habits meet. Cold Spring Harb Perspect Biol 7:a021691.
Gremel CM, Lovinger DM (2016) Associative and sensorimotor cortico-basal ganglia circuit roles in effects of abused drugs. Genes Brain Behav.
Grueter BA, Rothwell PE, Malenka RC (2012) Integrating synaptic plasticity and striatal circuit function in addiction. Curr Opin Neurobiol 22:545–551.
Hamilton DA, Kolb B (2005) Differential effects of nicotine and complex housing on subsequent experience-dependent structural plasticity in the nucleus accumbens. Behav Neurosci 119:355.
Heinsbroek JA, Neuhofer DN, Griffin 3rd WC, Siegel GS, Bobadilla AC, Kupchik YM, Kalivas PW (2017) Loss of plasticity in the D2-accumbens pallidal pathway promotes cocaine seeking. J Neurosci 37:757–767.
Holliday ED, Nucero P, Kutlu MG, Oliver C, Connelly KL, Gould TJ, Unterwald EM (2016) Long-term effects of chronic nicotine on emotional and cognitive behaviors and hippocampus cell morphology in mice: comparisons of adult and adolescent nicotine exposure. Eur J Neurosci.
Hsiang HL, Epp JR, van den Oever MC, Yan C, Rashid AJ, Insel N, Ye L, Niibori Y, Deisseroth K, Frankland PW, Josselyn SA (2014) Manipulating a ‘‘cocaine engram” in mice. J Neurosci 34:14115–14127.
Hyman SE (2005) Addiction: a disease of learning and memory. Am J Psychiatry 162:1414–1422.
Jedynak JP, Uslaner JM, Esteban JA, Robinson TE (2007) Methamphetamine-induced structural plasticity in the dorsal striatum. Eur J Neurosci 25:847–853.
Koob GF, Volkow ND (2010) Neurocircuitry of addiction. Neuropsychopharmacology 35:217–238.
Kravitz AV, Tye LD, Kreitzer AC (2012) Distinct roles for direct and indirect pathway striatal neurons in reinforcement. Nat Neurosci 15:816–818.
Kreitzer AC, Malenka RC (2008) Striatal plasticity and basal ganglia circuit function. Neuron 60:543–554.
Lee K, Holley SM, Shobe JL, Chong NC, Cepeda C, Levine MS, Masmanidis SC (2017) Parvalbumin Interneurons Modulate Striatal Output and Enhance Performance during Associative Learning. Neuron 93(1451–1463):e4.
Li J, Liu N, Lu K, Zhang L, Gu J, Guo F, An S, Zhang L, Zhang L (2012) Cocaine-induced dendritic remodeling occurs in both D1 and D2 dopamine receptor-expressing neurons in the nucleus accumbens. Neurosci Lett 517:118–122.
Lobo MK, Nestler EJ (2011) The striatal balancing act in drug addiction: distinct roles of direct and indirect pathway medium spiny neurons. Front Neuroanat 5.
Lobo MK, Zaman S, Damez-Werno DM, Koo JW, Bagot RC, DiNieri JA, Nugent A, Finkel E, Chaudhury D, Chandra R, Riberio E, Rabkin J, Mouzon E, Cachope R, Cheer JF, Han MH, Dietz DM, Self DW, Hurd YL, Vialou V, Nestler EJ (2013) DeltaFosB induction in striatal medium spiny neuron subtypes in response to chronic pharmacological, emotional, and optogenetic stimuli. J Neurosci 33:18381–18395.
McDonald CG, Dailey VK, Bergstrom HC, Wheeler TL, Eppolito AK, Smith LN, Smith RF (2005) Periadolescent nicotine administration produces enduring changes in dendritic morphology of medium spiny neurons from nucleus accumbens. Neurosci Lett 385:163–167.
McDonald C, Eppolito A, Brielmaier J, Smith L, Bergstrom H, Lawhead M, Smith R (2007) Evidence for elevated nicotine-induced structural plasticity in nucleus accumbens of adolescent rats. Brain Res 1151:211–218.
Nestler EJ (2004) Molecular mechanisms of drug addiction. Neuropharmacology 47:24–32.
NIDA (2014) https://www.drugabuse.gov/publications/drugs-brains-behavior-science-addiction/drug-abuse-addiction.
O’Brien C, McLellan AT (1996) Myths about the treatment of addiction. Lancet 347:237–240.
Ortega LA, Tracy BA, Gould TJ, Parikh V (2013) Effects of chronic low-and high-dose nicotine on cognitive flexibility in C57BL/6J mice. Behav Brain Res 238:134–145.
Pascual MM, Pastor V, Bernabeu RO (2009) Nicotine-conditioned place preference induced CREB phosphorylation and Fos expression in the adult rat brain. Psychopharmacology 207:57–71.
Perreault ML, Hasbi A, O’Dowd BF, George SR (2011) The dopamine D1-D2 receptor heteromer in striatal medium spiny neurons:

evidence for a third distinct neuronal pathway in basal ganglia. Front Neuroanat 5.
Picciotto MR, Zoli M, Rimondini R, Léna C, Marubio LM, Pich EM, Fuxe K, Changeux J (1998) Acetylcholine receptors containing the β2 subunit are involved in the reinforcing properties of nicotine. Nature 391:173–177.
Pontieri FE, Tanda G, Orzi F, Di Chiara G (1996) Effects of nicotine on the nucleus accumbens and similarity to those of addictive drugs. Nature 382:255.
Prager EM, Bergstrom HC, Grunberg NE, Johnson LR (2011) The importance of reporting housing and husbandry in rat research. Front Behav Neurosci 5:38.
Rice ME, Cragg SJ (2004) Nicotine amplifies reward-related dopamine signals in striatum. Nat Neurosci 7:583–584.
Robinson TE, Kolb B (2004) Structural plasticity associated with exposure to drugs of abuse. Neuropharmacology 47:33–46.
Russo SJ, Dietz DM, Dumitriu D, Morrison JH, Malenka RC, Nestler EJ (2010) The addicted synapse: mechanisms of synaptic and structural plasticity in nucleus accumbens. Trends Neurosci 33:267–276.
Schwabe L, Dickinson A, Wolf OT (2011) Stress, habits, and drug addiction: a psychoneuroendocrinological perspective. Exp Clin Psychopharmacol 19:53.
Smith KC, Ehlinger DG, Smith RF (2015a) Adolescent nicotine alters dendritic morphology in the bed nucleus of the stria terminalis. Neurosci Lett 590:111–115.
Smith RF, McDonald CG, Bergstrom HC, Ehlinger DG, Brielmaier JM (2015b) Adolescent nicotine induces persisting changes in development of neural connectivity. Neurosci Biobehav Rev 55:432–443.
Sowell ER, Thompson PM, Holmes CJ, Jernigan TL, Toga AW (1999) In vivo evidence for post-adolescent brain maturation in frontal and striatal regions. Nat Neurosci 2:859–861.
Spear LP (2016) Consequences of adolescent use of alcohol and other drugs: Studies using rodent models. Neurosci Biobehav Rev.
Stepanyants A, Chklovskii DB (2005) Neurogeometry and potential synaptic connectivity. Trends Neurosci 28:387–394.
Stuart G, Spruston N, Häusser M (2016) Dendrites. Oxford University Press.
Taylor S, Anglin J, Paode P, Riggert A, Olive M, Conrad C (2014) Chronic stress may facilitate the recruitment of habit-and addiction-related neurocircuitries through neuronal restructuring of the striatum. Neuroscience 280:231–242.
Valjent E, Hervé D, Girault J, Caboche J (2004) Addictive and non-addictive drugs induce distinct and specific patterns of ERK activation in mouse brain. Eur J Neurosci 19:1826–1836.
Voorn P, Vanderschuren LJ, Groenewegen HJ, Robbins TW, Pennartz CM (2004) Putting a spin on the dorsal–ventral divide of the striatum. Trends Neurosci 27:468–474.
Wang J, Cheng Y, Wang X, Roltsch Hellard E, Ma T, Gil H, Ben Hamida S, Ron D (2015) Alcohol elicits functional and structural plasticity selectively in dopamine D1 receptor-expressing neurons of the dorsomedial striatum. J Neurosci 35:11634–11643.
Yin HH, Knowlton BJ (2006) The role of the basal ganglia in habit formation. Nat Rev Neurosci 7:464–476.
Yin HH, Knowlton BJ, Balleine BW (2004) Lesions of dorsolateral striatum preserve outcome expectancy but disrupt habit formation in instrumental learning. Eur J Neurosci 19:181–189.
Yin HH, Knowlton BJ, Balleine BW (2006) Inactivation of dorsolateral striatum enhances sensitivity to changes in the action–outcome contingency in instrumental conditioning. Behav Brain Res 166:189–196.
Zhang H, Sulzer D (2004) Frequency-dependent modulation of dopamine release by nicotine. Nat Neurosci 7:581–582.

(Received 4 April 2017, Accepted 22 May 2017)
(Available online 31 May 2017)